PHYSICAL REVIEW C **91**, 054618 (2015)

Determination of ^{238}Pu(n, f) and ^{236}Np(n, f) cross sections using surrogate reactions

A. Pal,[*] S. Santra, B. K. Nayak, K. Mahata, V. V. Desai, and D. Chattopadhyay
Nuclear Physics Division, Bhabha Atomic Research Centre, Mumbai 400085, India

R. Tripathi
Radio Chemistry Division, Bhabha Atomic Research Centre, Mumbai 400085, India

(Received 12 November 2014; revised manuscript received 1 April 2015; published 29 May 2015)

The cross sections for ^{238}Pu(n,f) reaction for equivalent neutron energy of 13.0–22.0 MeV have been determined by the "surrogate ratio" method by measuring ^{235}U(^{6}Li$,df$) and ^{232}Th(^{6}Li$,df$) transfer induced fission reactions proceeding through the excited fissioning nuclei ^{239}Pu and ^{236}U, respectively, and using ^{235}U(n,f) cross-section data as the reference. Similarly, the cross sections for the ^{236}Np(n,f) reaction in the equivalent neutron energy range 9.9–22.0 MeV have been determined by the "hybrid surrogate ratio" method via the measurements of ^{235}U(^{6}Li$,\alpha f$) and ^{235}U(^{6}Li$,df$) transfer induced fission reactions, using ^{238}Pu(n,f) cross-section data as the reference. The EMPIRE-3.1 calculations for ^{238}Pu(n,f) and ^{236}Np(n,f) cross sections agree well with the present data, however, they are slightly underestimated by the ENDF/B-VII.1 evaluations.

DOI: 10.1103/PhysRevC.91.054618 PACS number(s): 24.87.+y, 25.70.Jj, 25.70.Hi, 25.85.Ge

I. INTRODUCTION

The study of neutron induced reactions on various targets not only provides a thorough understanding of the reaction mechanism of the formation and decay of compound nuclei but also has a tremendous potential in the applications in many areas of nuclear physics [1–8]. One of the important applications of neutron induced cross sections is its use in nuclear waste management programs. Fast neutron reactions have been proposed for the incineration of actinide materials, notably minor actinide isotopes which are produced in Th-U or U-Pu fuel cycles [2,3,6–8]. The spent fuel produced in the above cycles will be burned in a dedicated reactor, where neutron reactions such as (n,f) or (n,2n) can be used to reduce the content of radio-toxic isotopes. The neutron induced reactions play an extremely important role in astrophysical nucleo-synthesis [1,5].

Direct (n,f) cross-section measurements are sometimes very difficult because of the nonavailability of monoenergetic neutron beam and/or short half-lives of the target nuclei. Under these circumstances, the surrogate method first employed by Britt and Cramer in 1970 [9,10] is a well-celebrated method to measure the (n,f) cross sections indirectly. Later on, the "surrogate ratio (SR)" method was proposed by Plettner *et al.* [11] for the same purpose. Recently, the SR method was benchmarked and applied to determine several neutron induced fission cross sections [6,7,12–17]. Another method named "hybrid surrogate ratio (HSR)" method is also being used to determine the (n,f) cross sections as done in Ref. [6] by Nayak *et al.*

For the ^{236}Np(n,f) reaction, there is no experimental data on the fission cross section beyond 4.32 MeV available in the literature. So, we propose to measure two surrogate reactions and determine the above cross sections following the HSR method. To obtain the ^{236}Np(n,f) cross section in the ratio approach one needs to have the ^{238}Pu(n,f) cross section as a reference. Hence the cross sections for the ^{238}Pu(n,f) reaction have also been determined by measuring another set of surrogate reactions. However, in the second case the SR (instead of HSR) method was applied. For the ^{238}Pu(n,f) reaction, there exist some data by Resseler *et al.* [8] which were also obtained via the surrogate ratio approach. The present measurement aims to verify the literature data as well as extend the energy range for the (n,f) cross sections and finally use these cross sections as a reference to determine the ^{236}Np(n,f) cross sections.

The paper is organized in the following order. The surrogate methods in general and their use for determining the (n,f) cross sections for the present reactions are discussed in Sec. II. The experimental details and data analyses are described in Sec. III. Determinations of ^{238}Pu(n,f) and ^{236}Np(n,f) cross sections are described in Secs. IV and V, respectively. Finally the results are summarized in Sec. VI.

II. SURROGATE METHODS

The "surrogate" methods can be classified into three categories: (i) absolute surrogate method, (ii) surrogate ratio method, and (iii) hybrid surrogate ratio method. According to Bohr's theory, the decay of the compound nucleus (CN) is independent of the details of its entrance channel. If α is the entrance channel and β is the exit channel of a desired compound nuclear reaction,

$$\underbrace{a+A}_{\alpha} \longrightarrow C^{*} \longrightarrow \underbrace{b+B}_{\beta},$$

then the cross section for this reaction can be written as

$$\sigma_{\alpha\beta}(E_x)=\sum_{J\pi}\sigma_{\alpha}^{C}(E_x,J,\pi)G_{\beta}^{C}(E_x,J,\pi), \tag{1}$$

where $\sigma_{\alpha}^{C}(E_x,J,\pi)$ is the formation cross section of the compound nucleus "C" at excitation energy E_x, spin J, and parity π and $G_{\beta}^{C}(E_x,J,\pi)$ is the branching ratio for the decay

[*]asimpal@barc.gov.in

of this compound nucleus "C" into the desired exit channel β. The formation cross section can be calculated by using optical model potential with reasonable accuracy, but decay probability calculation is quite uncertain.

If the above experimental measurement is not possible because of the target instability or any difficulty in the generation of the beam, then according to surrogate strategy, one chooses an alternate reaction with stable target and stable beam that is easily available and produces the desired compound nucleus with the same excitation energy. It is then followed by the measurements of the required decay channels. So the objective of the surrogate method is to determine these decay probabilities via an indirect measurement. The independence hypothesis of the compound nucleus decay allows us to replace $\sigma_\alpha^C(E_x,J,\pi)$ in Eq. (1) by a factor representing any other reaction route that we expect to form an equilibrated compound nucleus. In a surrogate experiment the desired compound nucleus C is produced via a surrogate direct reaction,

$$\underbrace{d+D}_{\delta} \longrightarrow c + C^* \longrightarrow c + \underbrace{b+B}_{\beta},$$

and the decay of C is observed in coincidence with outgoing particle c. The formation probability of the desired compound nucleus "C" in this reaction is $F_\delta^C(E_x,J,\pi)$. The decay probability of the desired compound nucleus into β channel is given by

$$P_{\delta\beta}(E_x) = \sum_{J\pi} F_\delta^C(E_x,J,\pi) G_\beta^C(E_x,J,\pi). \tag{2}$$

Experimentally it can be obtained from the following equation.

$$P_{\delta\beta}^{\exp}(E_x) = \frac{N_{\delta\beta}}{N_\delta \epsilon_\delta}, \tag{3}$$

where $N_{\delta\beta}$ is the number of coincidences between the direct reaction particles c and one of the decay products b or B. N_δ represents the total number of surrogate events. ϵ_δ is the efficiency in detecting the decay products of C.

The surrogate method works under the Weisskopf-Ewing limit of the Hauser-Feschback theory [18,19] which says that the decay branching ratios are independent of J and π of the compound nucleus. So, in Eqs. (1) and (2) we can replace $G_\beta^C(E_x,J,\pi)$ by $G_\beta^C(E_x)$. Now, from Eq. (2) we get $P_{\delta\beta}(E_x) = G_\beta^C(E_x)$ because $\sum_{J\pi} F_\delta^C(E_x,J,\pi) = 1$. Consequently, combining Eqs. (1) and (3) we can write the expression for desired $\sigma_{\alpha\beta}(E_x)$ measured via the surrogate reaction (δ channel) as

$$\sigma_{\alpha\beta}^{(\delta)}(E_x) = \sigma_\alpha^{CN}(E_x)\frac{N_{\delta\beta}}{N_\delta \epsilon_\delta}. \tag{4}$$

This method is known as the absolute surrogate method. However, this method may sometimes introduce large errors to the (n,f) cross sections from the systematic uncertainties in the decay yield measurements as well as the model-calculated formation cross section for a single surrogate reaction. On the other hand, the surrogate ratio (SR) method is found to have an advantage over the absolute method. In the SR method, the ratio of the cross sections of two reactions with different target-projectile combinations are considered where the cross sections for one of the reactions are known and used as a reference. While taking the ratio of the decay probabilities of the composite nuclei formed by two different reactions many systematic uncertainties with respect to theory as well as experiment are removed. In the SR method, the dependence on J and π is shown to disappear at CN excitation energies higher than 8 MeV [11]. It is also shown that the ratio is insensitive to the pre-equilibrium effects for (n,f) reactions. There are several instances where the SR method was found to be valid at excitation energy even below 8 MeV. Applying the above surrogate technique Lyles *et al.* [13] have obtained the cross section for the ^{236}U(n,f) reaction which is comparable to the evaluated ENDF/B-VII data in the neutron energy range $E_n = 3.5$–20 MeV. The cross section below this energy, i.e., $E_n \leqslant 3.5$ MeV has the dependence on J^π of the compound nucleus. Similarly, Burke *et al.* [12] have obtained the cross sections for the ^{237}U(n,f) reaction by measuring the surrogate reactions ^{238}U$(\alpha,\alpha' f)$ and ^{236}U$(\alpha,\alpha' f)$ in the neutron energy range $E_n = 0$–20 MeV and the results are comparable (within the experimental uncertainty of 10%) to the previously measured data especially at low energy region ($E_n = 1$–10 MeV). Using the same SR method, Goldblum *et al.* [7] have determined the cross sections for ^{230,231}Th(n,f) reactions at energies $E_n = 0.22$–25.0 MeV and 0.36–10.0 MeV, respectively. The results agree with the directly measured data very well for the respective (n,f) reactions.

In the present study, we propose to obtain the cross section for the ^{238}Th(n,f) reaction using the above SR method by measuring two surrogate reactions, namely, ^{235}U(^{6}Li$,d)^{239}$Pu and ^{232}Th(^{6}Li$,d)^{236}$U at beam energies of 44.4 MeV. In both these reactions the exit channels are the same, i.e., deuterons are emitted. The number of outgoing deuterons along with the fission fragments of the residual composite nuclei (formed by the capture of α particles by the target) provides the probability of transfer induced fission decay channel. The excitation energies of the residual composite nuclei ^{239}Pu and ^{236}U formed in the above reactions are in the range of 18.6–27.6 MeV which is much higher than 8 MeV. So, the decay branching ratios are expected to be independent of J and π of the compound nucleus validating the Weisskopf-Ewing limit of the Hauser-Feschback theory. The reference reaction is taken to be the ^{235}U(n,f) reaction whose cross sections are available in the literature from the direct measurement by M. Cance *et al.* [20,21]. Now, the cross section for ^{238}Pu(n,f) reaction can be deduced from the following relation:

$$\frac{\sigma^{^{238}\mathrm{Pu}(n,f)}(E_x)}{\sigma^{^{235}\mathrm{U}(n,f)}(E_x)} = \frac{\sigma^{^{239}\mathrm{Pu}}(E_x)}{\sigma^{^{236}\mathrm{U}}(E_x)} \frac{N_{d-f}}{N_d} \frac{N_d^{'}}{N_{d-f}^{'}}. \tag{5}$$

Here, N_{d-f} and $N_{d-f}^{'}$ are the number of fission events occurring from the residual composite nuclei ^{239}Pu and ^{236}U, respectively, measured in coincidence with the deuterons (produced in the direct reactions). The corresponding inclusive deuteron yields are denoted by N_d and $N_d^{'}$, respectively. The compound nuclear formation cross sections in $n+{}^{235}$U $\rightarrow$ ^{236}U and $n+{}^{238}$Pu $\rightarrow$ ^{239}Pu reactions at excitation energy E_x

are denoted by $\sigma^{^{236}\mathrm{U}}(E_x)$ and $\sigma^{^{239}\mathrm{Pu}}(E_x)$, respectively, whose values are obtained from the EMPIRE calculations.

In the third method, i.e., the hybrid surrogate ratio (HSR) method, two reactions are chosen from the same target-projectile combination. Two different reaction channels considered here, e.g., (^{6}Li ,αf) and (^{6}Li ,df) when ^{6}Li is a projectile. The choice of target-projectile combination is made in such a way that the above transfer reactions populate two nearby residual composite nuclei at the same excitation energies. However, the distribution of the angular momenta of the respective composite nuclei populated by the capture of deuteron in the first reaction and α in the second reaction may be different. In general, the assumption of the independence of J and π in the calculation of the decay probability "$G_\beta^C(E_x,J,\pi)$" may not be true and in that case the HSR method cannot be applied. Therefore, one has to verify the validity of the above assumption for the concerned composite nuclei at the excitation energies formed by two surrogate reactions before this method can be applied to determine the corresponding (n,f) cross section.

In the second set of present measurements, we propose to determine the ^{236}Np(n,f) cross section using the HSR method by measuring two surrogate reactions ^{235}U(^{6}Li ,α)^{237}Np and ^{235}U(^{6}Li ,d)^{239}Pu. Two residual composite nuclei (^{237}Np and ^{239}Pu) formed in the above two transfer reactions are the same as the compound nuclei formed in the $n+{}^{236}$Np and $n+{}^{238}$Pu reactions, respectively. The ground-state Q values (Q_{gg}) for these two surrogate reactions are 7.70 MeV and -6.72 MeV, respectively. From the excitation energy calculation of a transfer reaction [$E_x = Q_{gg} - Q_{\rm opt}$; $Q_{\rm opt} = E_{\rm cm}(\frac{z_{1f}z_{2f}}{z_{1i}z_{2i}} - 1)$] it can be noticed that the residual composite nuclei ^{237}Np and ^{239}Pu can be populated at overlapping excitation energies for two transfer channels when ^{6}Li is incident on ^{235}U with bombarding energy of $\sim$44.4 MeV. The spin distribution of the two composite nuclei, formed by ^{235}U(^{6}Li ,α) and ^{235}U(^{6}Li ,d) reactions, respectively, are different though. The overlapping excitation energy of two composite nuclei is in the range of $\sim$16$-$28 MeV. At such excitation energies, the level density of the residual composite nuclei is very high and the fission decay probability will be independent of the angular momentum acquired by capturing the breakup/transferred fragment. But, the effect of J on fission decay probability can be significant for the higher chance fissions, e.g., $(n,2nf)$ or $(n,3nf)$ decays where the excitation energy available at the fission saddle point is very low. Assuming breakup of the projectile or transfer reaction is from peripheral collisions and the energy of deuteron (alpha) is equal to one-third (two-thirds) of the beam energy, the angular momentum involved in ^{235}U(^{6}Li ,α)^{237}Np and ^{235}U(^{6}Li ,d)^{239}Pu reactions are calculated to be $J \sim 11\hbar$ and $23\hbar$, respectively. To investigate the dependence of J on fission decay probability in ^{236}Np(n,f) and ^{238}Pu(n,f) reactions detailed calculations using the EMPIRE code [22] Version 3.1, have been performed at neutron energy in the range of $E_n = 1$–23 MeV. The results of the above calculations for $J = 5\hbar, 15\hbar$, and $25\hbar$ are shown as dashed, dash-dot-dot, and solid line, respectively, in Fig. 1. As the neutron energy E_n increases beyond 10 MeV (the region of our interest), it

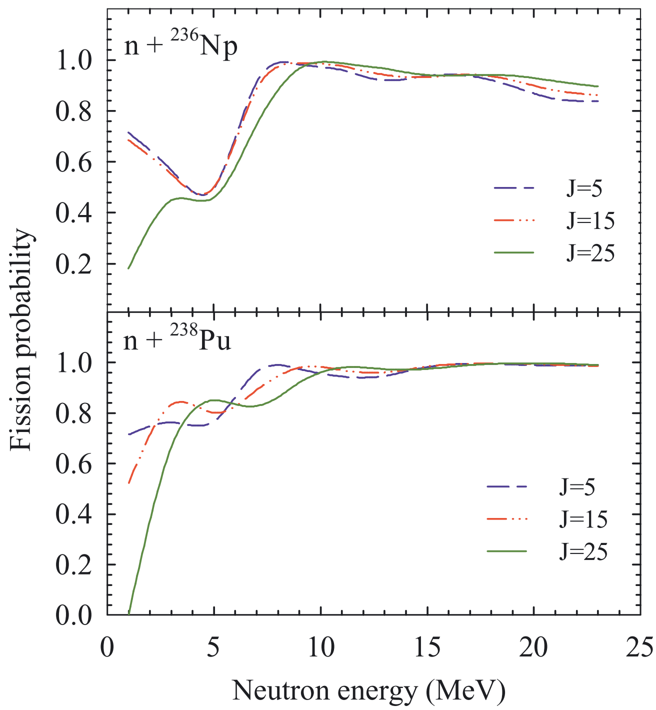

FIG. 1. (Color online) Fission decay probability in ^{236}Np(n,f) (upper panel) and ^{238}Pu(n,f) (lower panel) reactions calculated using the EMPIRE code as a function of neutron energy with different compound-nucleus J values.

can be observed that the difference in the fission probabilities corresponding to a $\Delta J \sim 10\hbar$ narrows down to $\leqslant 5\%$. Thus, the decay probabilities of the present composite nuclei have little dependence on the initial distribution of J. Hence, if we assume that the fission probability of the compound nucleus as a function of angular momentum is accurately reproduced via the EMPIRE reaction model, one can use the HSR method to obtain the (n,f) cross section from the above surrogate reactions within a small uncertainty contributed by the spin mismatch of the composite nuclei.

So, we can now use Eq. (4) and write the expression for the ^{236}Np(n,f) reaction cross section as

$$\frac{\sigma^{^{236}\mathrm{Np}(n,f)}(E_x)}{\sigma^{^{238}\mathrm{Pu}(n,f)}(E_x)} = \frac{\sigma^{^{237}\mathrm{Np}}(E_x)}{\sigma^{^{239}\mathrm{Pu}}(E_x)} \frac{N_{\alpha-f}}{N_\alpha} \frac{N_d}{N_{d-f}}. \tag{6}$$

Here, $N_{\alpha-f}$ and N_{d-f} correspond to the number of fission events measured in coincidence with outgoing direct reaction products α and d particles, respectively. The inclusive α and d counts are denoted by N_α and N_d, respectively. The compound nuclear formation cross sections $\sigma^{^{237}\mathrm{Np}}(E_x)$ and $\sigma^{^{239}\mathrm{Pu}}(E_x)$ at excitation energy E_x, in the reaction $n+{}^{236}\mathrm{Np} \rightarrow {}^{237}$Np and $n+{}^{238}\mathrm{Pu} \rightarrow {}^{239}$Pu, respectively, are obtained from the EMPIRE calculations. The cross sections for the ^{238}Pu(n,f) reaction can be used as a reference which can either be obtained from the present measurements described above and/or the available indirect measurement by Ressler *et al.* [8].

III. EXPERIMENT AND DATA ANALYSIS

Measurements were carried out using the 44.4-MeV ^{6}Li beam from the BARC-TIFR Pelletron accelerator facility in Mumbai. Targets used are (i) 1.6-mg/cm^2 thick ^{235}U electrodeposited on 4.5-mg/cm^2 thick Ni-Cu backing and (ii) 1.3-mg/cm^2 thick self-supported ^{232}Th target. One telescope ($\Delta E - E$) made of silicon surface barrier detectors, used to detect light charged particles, was kept at an 80° angle with respect to the beam direction, when the ^{235}U target was used. To study the other reaction (^{6}Li+ ^{232}Th) the telescope was kept at a 70° angle with respect to beam direction because of the lower grazing angle compared to the previous one. An aluminium foil of thickness ~6.75 mg/cm^2 was placed in front of the particle telescope to stop the fission fragments entering the ΔE detector and prevent it from radiation damage. A ^{229}Th alpha source was used to calibrate the ΔE and E silicon detectors. Distance between each telescope and target was 18.6 cm. A large area silicon detector (with a solid angle ~33 msr and an angular coverage of 154°–166°) was used to detect fission fragments in the backward hemisphere. The fission detector was placed at a distance of 11 cm from the target center. Two monitor detectors were placed at forward angles to monitor the stability of the beam. Particles were identified from the ΔE vs (ΔE+E) plot. Because the particles reach the detectors after losing energy through Ni-Cu backing and aluminium foil, the respective energy losses have been calculated using the SRIM program [23] and the actual energy of the outgoing light charged particle was reconstructed event by event.

Reactions with only Ni-Cu backing have been separately studied and light charged particle contributions from the Ni-Cu backing have been estimated. As shown in Fig. 2 alpha and deuteron contributions (blue line) in the telescope from the Ni-Cu backing have been subtracted out from the total (pink line) contribution (^{235}U + Ni-Cu backing) resulting in the pure alpha and deuteron contribution from ^{235}U target (green line). While subtracting the contribution of the target backing, the relative shift in the energy spectra from uranium thickness was taken into account.

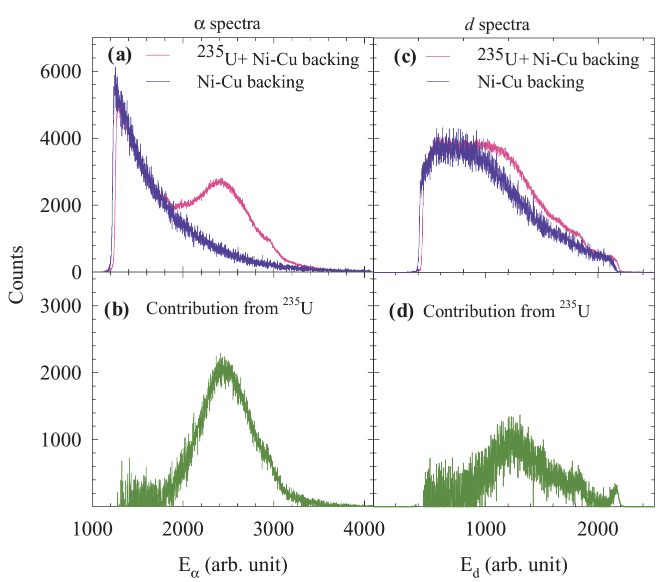

FIG. 2. (Color online) Typical alpha and deuteron spectra from ^{235}U + Ni-Cu backing (pink line) and only Ni-Cu backing (blue line) are shown in (a) and (c). Corresponding spectra only from ^{235}U target (green line) obtained from the difference of the above two contributions are shown in (b) and (d), respectively.

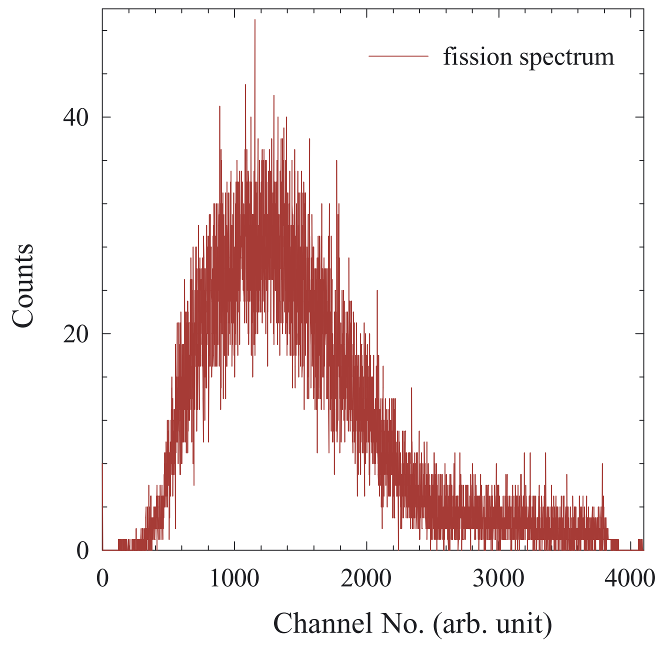

FIG. 3. (Color online) Typical fission spectrum obtained in coincidence with light charged particles in ^{6}Li+ ^{235}U reaction.

The time correlation between light charged particles and fission fragments was recorded through a time-to-amplitude converter (TAC). A typical fission spectrum obtained in coincidence with the light charged particle in the ^{6}Li+ ^{235}U reaction was shown in Fig. 3.

IV. DETERMINATION OF ^{238}Pu (n, f) CROSS SECTION

First we determined the cross sections for the ^{238}Pu(n, f) reaction using the surrogate ratio (SR) method. These results, along with the data available from the literature, were later used as the reference reaction cross sections for determining the cross section of the ^{236}Np(n, f) reaction using the HSR method. The experimental data from the present measurements for ^{235}U(^{6}Li ,df) and ^{232}Th(^{6}Li ,df) transfer induced fission reactions which proceed through the excited fissioning nuclei ^{239}Pu and ^{236}U, respectively, were analyzed. The excitation energy of the desired composite nucleus formed in the transfer reaction is calculated using the relation $E_x = (E_{\text{beam}} - E_{\text{out}} - E_{\text{recoil}}) + Q$, where E_{out} is the energy of the outgoing particle, E_{recoil} is the recoil energy of the compound nucleus calculated from the recoil momentum, and Q is the Q value of the reaction.

If S_n is the neutron separation energy from a compound nucleus with mass number A and excitation energy E_x, the equivalent neutron energy can be written as $E_n = \frac{A}{A-1}(E_x - S_n)$. Neutron separation energies for the compound nuclei ^{236}U and ^{239}Pu are 6.54 MeV and 5.65 MeV, respectively, using which the equivalent neutron energies are calculated.

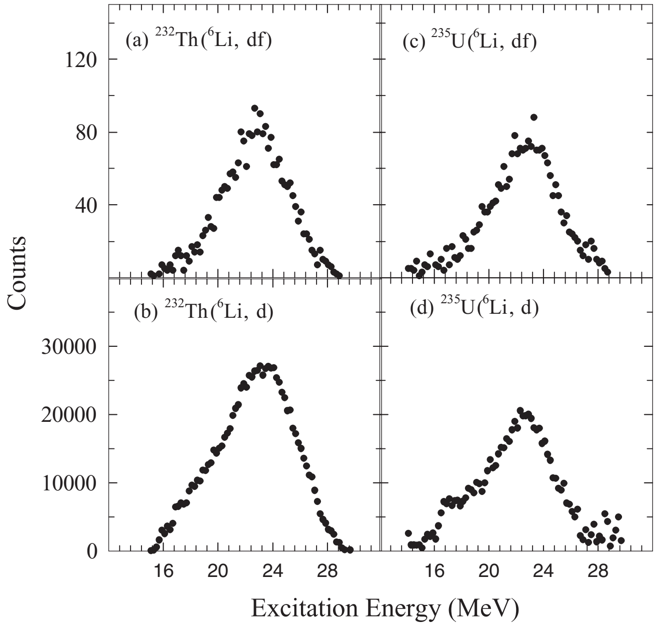

FIG. 4. Deuteron spectra for (a) and (b) ^{232}Th(^{6}Li,d)^{236}U, and (c) and (d) ^{235}U(^{6}Li,d)^{239}Pu transfer reactions, respectively. Deuterons measured in coincidence with fission fragments for the respective reactions are shown in (a) and (c) and those in singles are shown in (b) and (d). Background from the Ni-Cu backing is subtracted.

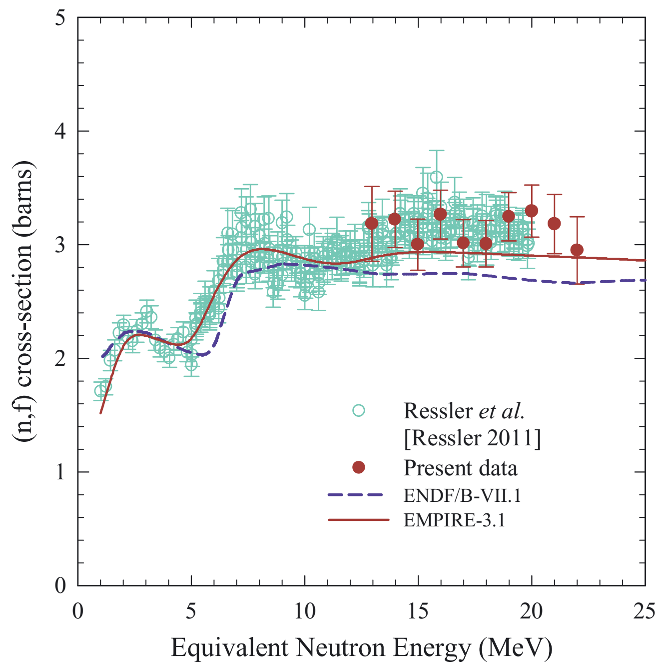

FIG. 5. (Color online) Determined ^{238}Pu(n,f) cross sections (solid circle) along with the data (hollow circle) measured by Ressler *et al.* [8]. Solid and dashed lines correspond to the results of EMPIRE calculations and ENDF/B-VII.1 evaluations, respectively.

Figure 4 shows the deuteron spectra obtained from ^{232}Th(^{6}Li,d)^{236}U and ^{235}U(^{6}Li,d)^{239}Pu reactions. The deuterons measured in coincidence with the fission fragments for the above two reactions correspond to the spectra of Figs. 4(a) and 4(c), respectively, whereas the deuterons measured in singles correspond to Figs. 4(b) and 4(d) respectively. In the spectra shown for the ^{235}U(^{6}Li,d)^{239}Pu reaction, the background from the Ni-Cu backing was already subtracted.

Following the expression given in Eq. (5), which was obtained from the SR method, the cross sections for the ^{238}Pu(n,f) reaction have been determined in the equivalent neutron energy range of 13.0–22.0 MeV. The results are shown in Fig. 5 as solid circles. The data measured by Ressler *et al.* [8] are also shown in the figure as hollow circles. The data from the present measurements are found to be in good agreement with the ones by Ressler *et al.* in the overlapping energy region. Hence, one can now use the present ^{238}Pu(n,f) cross sections along with the literature data as the reference to determine the ^{236}Np(n,f) cross sections by the HSR method.

The results of the ENDF/B-VII.1 evaluations for ^{238}Pu(n,f) cross sections have also been shown in Fig. 5 as a dashed line. It can be observed that the evaluated cross sections reproduce the low energy data very well but slightly underestimate the high energy data.

The EMPIRE calculations have been carried out to quantitatively understand the ^{238}Pu(n,f) cross section over the neutron energy range 1.0–25.0 MeV. The decay probabilities of the compound nuclei up to fourth chance fission, i.e., the decay of ^{239,238,237,236}Pu nuclei have been included. The inner (V_a) and outer (V_b) fission barrier parameters of a double humped fission barrier for the ^{239,238,237}Pu isotopes have been taken from the Reference Input Parameter Library (RIPL-3) [24] which is a standard library of fission barrier parameters for actinides. The required fission barrier heights for the ^{236}Pu isotope is not available in RIPL-3. Hence it was calculated from the barrier formula (BF) as given in Ref. [17]. The final calculations have been made after slight modifications of the barrier parameters to explain the measured (n,f) cross sections. The initial and final barrier parameters are given in Table I. The results of the EMPIRE calculations with modified barrier parameters are shown as a solid line in Fig. 5.

V. DETERMINATION OF ^{236}Np(n,f) CROSS SECTION

Here, we analyze the raw data for ^{235}U(^{6}Li,αf) and ^{235}U(^{6}Li,df) transfer induced fission reactions which proceed through excited fissioning nuclei ^{237}Np and ^{239}Pu, respectively. The excitation energies of the desired compound nuclei have been obtained following the same procedure mentioned

TABLE I. Barrier heights used for Pu isotopes in EMPIRE-3.1 calculations.

Isotopes	Standard		Modified	
	V_a	V_b	V_a	V_b
^{239}Pu	6.20[a]	5.70[a]	6.40	5.80
^{238}Pu	5.60[a]	5.10[a]	5.60	5.10
^{237}Pu	5.10[a]	5.15[a]	4.50	4.15
^{236}Pu	5.71[b]	4.91[b]	4.70	4.90

[a]RIPL [24].
[b]BF [17].

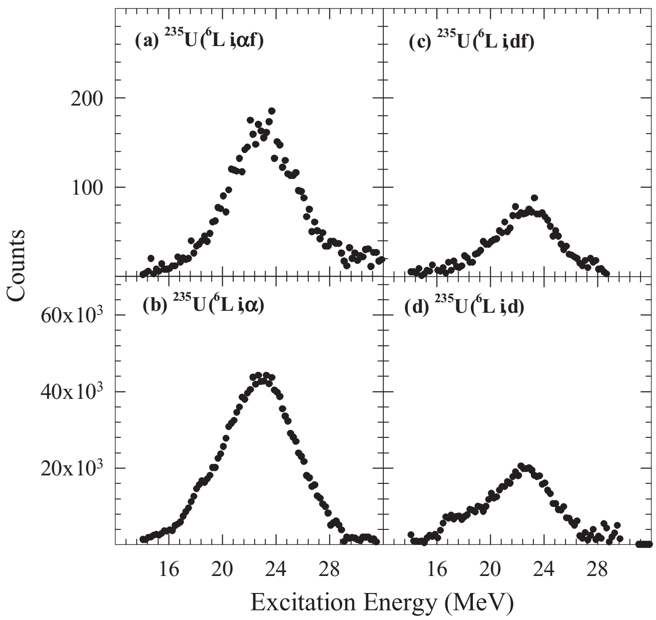

FIG. 6. Coincident and inclusive spectra for (a) and (b) alpha, and (c) and (d) deuteron, respectively, in the ^{6}Li+ ^{235}U reaction.

earlier. Overlapping excitation energies of ^{237}Np and ^{239}Pu desired compound nuclei have been found to be in the range of 16.6–28.6 MeV. The inclusive as well as exclusive (in coincidence with fission) spectra for alpha and deuteron yields obtained from the above two reactions are shown in Fig. 6. Neutron separation energies for the compound nuclei ^{237}Np and ^{239}Pu are 6.57 MeV and 5.65 MeV, respectively, using which the equivalent neutron energies are calculated. The

TABLE II. Barrier heights used for Np isotopes in EMPIRE-3.1 calculation.

Isotopes	Standard		Modified	
	V_a	V_b	V_a	V_b
^{237}Np	6.00[a]	5.40[a]	6.45	5.40
^{236}Np	5.90[a]	5.40[a]	5.90	5.40
^{235}Np	5.88[b]	5.51[b]	6.30	5.70
^{234}Np	6.20[b]	5.68[b]	6.40	5.70

[a]RIPL [24].
[b]BF [17].

excitation energy of the residual composite nuclei and the equivalent neutron energy have been calculated using the expression mentioned in the previous section for every 1 MeV bin of the spectra. Now using the formula mentioned in Eq. (6) the desired reaction cross sections have been determined for equivalent neutron energy in the range of 9.9–22.0 MeV (Fig. 7).

The EMPIRE calculations for the ^{236}Np(n,f) cross section have been carried out at the neutron energy in the range of $E_n = 1.0$–24.0 MeV. Similar to the ^{238}Pu(n,f) reaction, the calculations for the present system also consider the decay of the compound nuclei up to fourth chance fission, i.e., the decay of ^{237,236,235,234}Np nuclei. The initial barrier parameters for ^{237}Np and ^{236}Np isotopes have been taken from RIPL-3 and those for the ^{235}Np and ^{234}Np isotopes have been calculated from the barrier formula (BF) [17]. Modified barrier parameters have been used to get a best fit

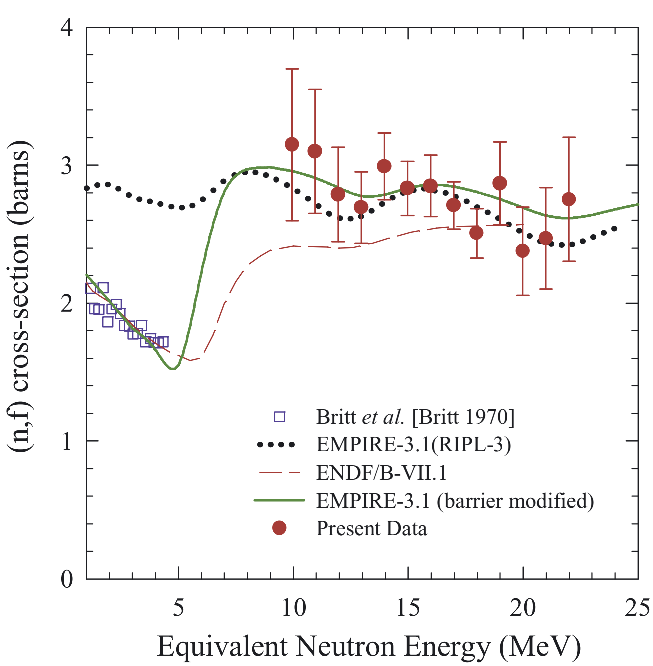

FIG. 7. (Color online) ^{236}Np(n,f) cross section as a function of equivalent neutron energy. Open squares are the existing data measured by Britt *et al.* [9]. Dotted and solid lines represent the EMPIRE-3.1 calculations.

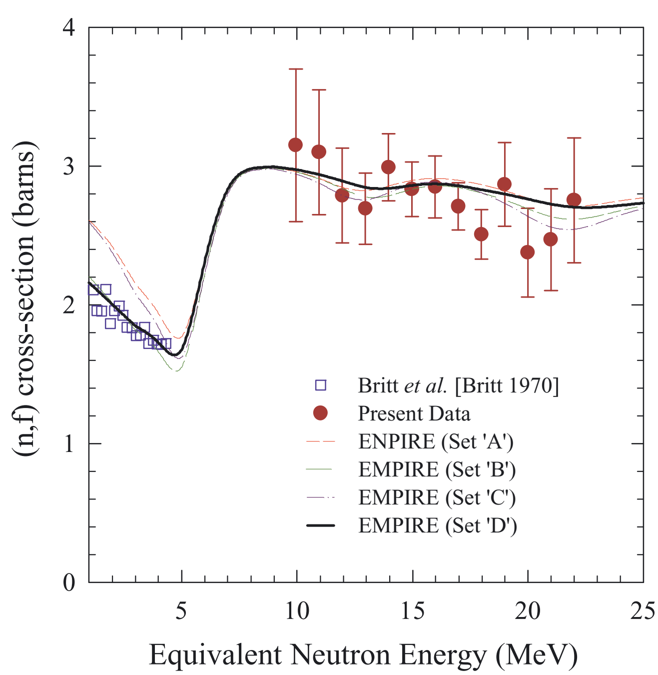

FIG. 8. (Color online) EMPIRE predictions for ^{236}Np(n,f) cross section as a function of neutron energy using four different sets of parameters of nuclear level density and fission barriers. Open squares are the existing data measured by Britt *et al.* [9]. Dotted and solid lines represent the EMPIRE-3.1 calculations.

TABLE III. Different sets of parameters on fission barriers and level density of the residual composite nuclei used in EMPIRE calculations to see the sensitivity of these parameters.

Set	Fission barriers	Level density	Line type
A	Default	Default	Short-dashed
B	Modified (same as Table II)	Default	Long-dashed
C	Default	Increased by 5%	Dash-dotted
D	Modified	Decreased by 5%	Solid

to the experimental data. The initial and final fission barrier parameters used in these calculations are given in Table II. The EMPIRE calculations with the initial as well as the modified barrier parameters (dotted and solid lines) reproduce the present data for ^{236}Np(n,f) very well within the experimental uncertainty. However, a reduced value of the "Kdis" parameter [from 6.0 (default) to 2.5] of the discrete transitional state of the ^{236}Np nucleus was used in the EMPIRE calculations to reproduce both the low energy data of Ref. [9] as well as the present data (solid line). The ^{236}Np(n,f) cross sections were also evaluated using ENDF/B-VII.1 (dashed line) which are found to be in good agreement with the low energy data measured by Britt *et al.* [9], but they are slightly underpredicted compared to the present data (Fig. 7) at intermediate energies.

To explain the measured data on the (n,f) cross sections, the EMPIRE calculations so far have been made by adjusting only the fission barrier parameters of the residual composite nuclei. To look for the sensitivity of the (n,f) cross section to other parameters, e.g., level density of the composite nuclei, the EMPIRE calculations have been carried out using several combinations of input parameters on fission barriers as well as level density that provide reasonable reproduction of the measured cross sections. Figure 8 shows the results of the above calculations for the ^{236}Np(n,f) cross section with four sets of parameters (set "A"–"D") as described in Table III. Comparing the EMPIRE results with parameter set "A" (default values) to those for set "B" (modified barriers) and "C" (modified level density) one can find that the (n,f) cross sections are more sensitive to the fission barrier parameters than the level density, particularly at neutron energies $E_n \leqslant 5$ MeV. Best results, as represented by a long dashed line and a solid line in Fig. 8, have been obtained, respectively, with parameter set "B" with modified barriers and set "D" with modified level density as well as fission barriers. In set "D," the level density was reduced by 5% and accordingly the fission barriers have been readjusted (slightly different from Table I) to get the best fit to the present data at high energy as well as the literature data at low energy.

VI. SUMMARY

The fission fragments emitted at backward angles are measured in coincidence with the light charged particles emitted around the grazing angles for ^{6}Li+ ^{235}U , ^{232}Th reactions at a bombarding energy of 44.4 MeV. Surrogate methods have been used to obtain the neutron induced fission cross sections for ^{238}Pu and ^{236}Np target nuclei at neutron energies in the range of ~9.9–22.0 MeV. The cross sections for the ^{238}Pu(n,f) reaction have been determined for equivalent neutron energy of 13.0–22.0 MeV employing the "surrogate ratio" method in which the ratio of the exclusive (coincidence) to inclusive (singles) yields of the light charged particles measured in two reaction channels, i.e., ^{235}U(^{6}Li ,*df*) and ^{232}Th(^{6}Li ,*df*) is used. The ^{235}U(n,f) reaction, for which the cross-section data is available in the literature, was used as a reference reaction. The cross sections thus obtained for the ^{238}Pu(n,f) reaction are found to be in good agreement with the data available in the literature at the overlapping energy region.

Similarly, the cross sections for the ^{236}Np(n,f) reaction have been determined for equivalent neutron energy of 9.9–22.0 MeV employing the "hybrid surrogate ratio" method where the yields from two other reaction channels, i.e., ^{235}U(^{6}Li ,αf) and ^{235}U(^{6}Li ,*df*) reactions have been used. The reference reaction for the above method was chosen to be the ^{238}Pu(n,f) reaction for which the cross sections from the literature along with the ones obtained from the present measurements are utilized.

The EMPIRE calculations with default as well as modified parameters are found to reproduce the present data for ^{236}Np(n,f) cross sections very well. However, the calculations with default parameters do not reproduce the literature data at low energy. A reduced value of the "Kdis" parameter of the discrete transitional state of the ^{236}Np nucleus, from 6.0 (default) to 2.5, is found to provide a good description of both low as well as high energy data. The calculations also show that the (n,f) cross sections are more sensitive to fission barrier parameters than to the level density parameters of the compound nuclei. The ENDF/B-VII.1 evaluated cross- sections for both ^{238}Pu(n,f) and ^{236}Np(n,f) reactions are found to be in good agreement with the data at low energies but they are on an average slightly lower compared to the present cross sections in the measured energy range. An improvement in the ENDF evaluations may be required for a consistent description of the above (n,f) cross sections for the entire energy range of the experimental data.

ACKNOWLEDGMENT

The authors would like to thank the pelletron crew for the smooth operation of the accelerator during the experiments.

[1] S. Goriely and M. Arnould, Astron. Astrophys. **379**, 1113 (2001).

[2] M. Petit, M. Aiche, G. Barreau, S. Boyer, N. Carjan, S. Czajkowski, D. Dassie, C. Grosjean, A. Guiral, B. Haas *et al.*, Nucl. Phys. A **735**, 345 (2004).

[3] S. Boyer, D. Dassie, J. N. Wilson, M. Ache, G. Barreau, S. Czajkowski, C. Grosjean, A. Guiral, B. Haas, B. Osmanov *et al.*, Nucl. Phys. A **775**, 175 (2006).

[4] G. Alibarti, G. Palmiotti, M. Salvatores, T. Kim, T. Taiwo, M. Anitescu, I. Kodeli, E. Sartori, J. Bosq, and J. Tommasi, Ann. Nucl. Energy **33**, 700 (2006).

[5] G. Wasserburg, M. Busso, R. Gallino, and K. Nollett, Nucl. Phys. A **777**, 5 (2006).
[6] B. K. Nayak, A. Saxena, D. C. Biswas, E. T. Mirgule, B. V. John, S. Santra, R. P. Vind, R. K. Choudhury, and S. Ganesan, Phys. Rev. C **78**, 061602(R) (2008).
[7] B. L. Goldblum, S. R. Stroberg, J. M. Allmond, C. Angell, L. A. Bernstein, D. L. Bleuel, J. T. Burke, J. Gibelin, L. Phair, N. D. Scielzo *et al.*, Phys. Rev. C **80**, 044610 (2009).
[8] J. J. Ressler, J. T. Burke, J. E. Escher, C. T. Angell, M. S. Basunia, C. W. Beausang, L. A. Bernstein, D. L. Bleuel, R. J. Casperson, B. L. Goldblum *et al.*, Phys. Rev. C **83**, 054610 (2011).
[9] H. C. Britt and J. D. Cramer, Phys. Rev. C **2**, 1758 (1970).
[10] J. D. Cramer and H. C. Britt, Phys. Rev. C **2**, 2350 (1970).
[11] C. Plettner, H. Ai, C. W. Beausang, L. A. Bernstein, L. Ahle, H. Amro, M. Babilon, J. T. Burke, J. A. Caggiano, R. F. Casten *et al.*, Phys. Rev. C **71**, 051602(R) (2005).
[12] J. T. Burke, L. A. Bernstein, J. Escher, L. Ahle, J. A. Church, F. S. Dietrich, K. J. Moody, E. B. Norman, L. Phair, P. Fallon *et al.*, Phys. Rev. C **73**, 054604 (2006).
[13] B. F. Lyles, L. A. Bernstein, J. T. Burke, F. S. Dietrich, J. Escher, I. Thompso, D. L. Bleuel, R. M. Clark, P. Fallon, J. Gibelin *et al.*, Phys. Rev. C **76**, 014606 (2007).
[14] S. R. Lesher, J. T. Burke, L. A. Bernstein, H. Ai, C. W. Beausang, D. L. Bleuel, R. M. Clark, F. S. Dietrich, J. E. Escher, P. Fallon *et al.*, Phys. Rev. C **79**, 044609 (2009).
[15] R. O. Hughes, C. W. Beausang, T. J. Ross, J. T. Burke, N. D. Scielzo, M. S. Basunia, C. M. Campbell, R. J. Casperson, H. L. Crawford, J. E. Escher *et al.*, Phys. Rev. C **85**, 024613 (2012).
[16] A. Czeszumska, C. T. Angell, J. T. Burke, N. D. Scielzo, E. B. Norman, R. A. E. Austin, G. Boutoux, R. J. Casperson, P. Chodash, R. O. Hughes *et al.*, Phys. Rev. C **87**, 034613 (2013).
[17] V. V. Desai, B. K. Nayak, A. Saxena, D. C. Biswas, E. T. Mirgule, B. John, S. Santra, Y. K. Gupta, L. S. Danu, G. K. Prajapati *et al.*, Phys. Rev. C **87**, 034604 (2013).
[18] V. F. Weisskopf and D. H. Ewing, Phys. Rev. **57**, 472 (1940).
[19] J. E. Escher, J. T. Burke, F. S. Dietrich, N. D. Scielzo, I. J. Thompson, and W. Younes, Rev. Mod. Phys. **84**, 353 (2012).
[20] M. Cance and G. Grenier, Nucl. Sci. Engg. **68**, 197 (1978).
[21] M. Cance, G. Grenier, D. Gimat, and D. Parisot, http://www.nndc.bnl.gov/EXFOR/20779.002 (EXFOR database version October 13, 2014).
[22] M. Herman, R. Capote, B. Carlson, P. Oblozinsky, M. Sin, A. Trkov, H. Wienke, and V. Zerkin, Nucl. Data Sheets **108**, 2655 (2007).
[23] J. Ziegler, Computer code srim, 2013 http://www.srim.org/.
[24] R. Capote, M. Herman, P. Oblozinsky, P. Young, S. Goriely, T. Belgya, A. Ignatyuk, A. Koning, S. Hilaire, V. Plujko *et al.*, Nucl. Data Sheets **110**, 3107 (2009).